論文 / 著書情報
Article / Book Information

Title	ACCURACY OF PREDICTION FORMULA FOR DAMAGE CAUSING ENERGY BY HYSTERETIC DAMPER
Authors	Jing LI, Daiki SATO
Pub. date	2020, 11
Citation	Proceedings of the 15th Annual Meeting of Japan Association for Earthquake Engineering

ACCURACY OF PREDICTION FORMULA FOR DAMAGE CAUSING ENERGY BY HYSTERETIC DAMPER

Jing LI[1], Daiki SATO[2]

[1] Graduate Student, Dept. of Architectural Engineering, Tokyo Institute of Technology, Tokyo, Japan, li.j.bd@m.titech.ac.jp
[2] Associate professor, Institute of Innovative Research, Tokyo Institute of Technology, Tokyo, Japan, sato.d.aa@m.titech.ac.jp

ABSTRACT: Akiyama proposed a prediction formula indicated the relationship between the total energy input and the energy input that contributes to damage. This formula can be used to calculate the equivalent velocity of energy combined with earthquake ground response spectrum. The object of this paper is to discuss the accuracy of the prediction formula for energy caused by hysteretic damper. According to the results, verification of the proposed formula indicates good accuracy for artificially generated earthquake ground motions.

Keywords: SDOF Model, Energy Balance, Response Prediction Method, Equivalent Velocity

1. INTRODUCTION

The isolation structure showed the benefits of restraining the damage of the mainframe and being easy to repair after an earthquake comparing with the aseismic structure. Therefore, the number of isolation structures has increased year by year. Especially in recent years, the possibility of huge earthquakes is extremely high, so the research on isolation structures has become more and more significant. Various studies have been carried out on isolation structure, response prediction method base on energy balance, proposed by Akiyama[1)], is generally used to predict the response of isolation structure because of sufficient reliability and convenience. In Akiyama's response prediction research, Akiyama proposed a formula that showed the relationship between V_E and V_D. Here, V_E is an equivalent velocity of the total input energy and V_D is an equivalent velocity of the energy input that contributes to damage. This formula can be used to calculate the equivalent velocity, which combined with the earthquake ground response spectrum.

In Akiyama's research of response prediction, the observed earthquake records, the El centro, Hachinohe, and Long Beach, are adopted as ground motions, to verify the prediction formula by time history analysis. However, the artificially generated earthquake ground motions are used to seismic design recently. Therefore, the accuracy of the prediction formula should be verified by using not only the observed earthquake records but also the artificially generated earthquake ground motions.

The object of this paper is to discuss accuracy of prediction formula for energy caused by hysteretic damper. In this paper, artificially generated earthquake ground motions are be adopted to calculate response of a single degree of freedom (SDOF) isolation structure by time history analysis. The results show that, almost errors of cases, less than 20%. Therefore, it seems to be satisfactory accurate according to preliminary verification for artificially generated earthquake ground motions.

2. OUTLINE OF ANALYSIS MODEL AND GROUND MOTIONS

2.1 OUTLINE OF ANALYSIS MODEL

Figure 1 shows an analysis model of the isolation structure for the SDOF model. The system consists of an isolation layer and a hysteretic damper. The isolation layer supports the gravity of the building and is in elastic deformation. The hysteretic damper that absorbs seismic energy presents elastic-plastic behavior. Here, c_f represents the viscous damping coefficient, k_f represents the stiffness of isolation layer, k_d represents the stiffness of hysteretic damper, α_f represents the shear force coefficient of isolation layer and α_{dy} represents the yield shear force coefficient of isolation layer. In addition, $_f$ represents the isolation layer and $_d$ represents the hysteretic damper.

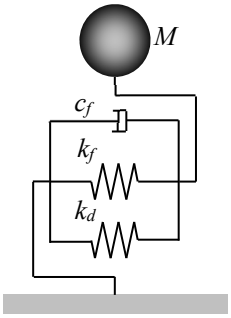

Fig. 1 Analysis Model of isolation structure

Figure 2 shows the restoring force characteristic of model. Here, (a) is the restoring force characteristic of the isolation layer, (b) is the restoring force characteristic of the hysteretic damper, (c) is the restoring force characteristic of the viscous damping, and (d) is the restoring force characteristic of the system, respectively. Here, $Q_{f\max}$: Maximum shear force of isolator, Q_{dy}: Yield shear force of hysteretic damper, α_{dy} : yield shear force coefficient of hysteretic damper, $\delta_{\max}$: Maximum deformation of isolation layer, and δ_{dy}: Yield deformation of hysteretic damper

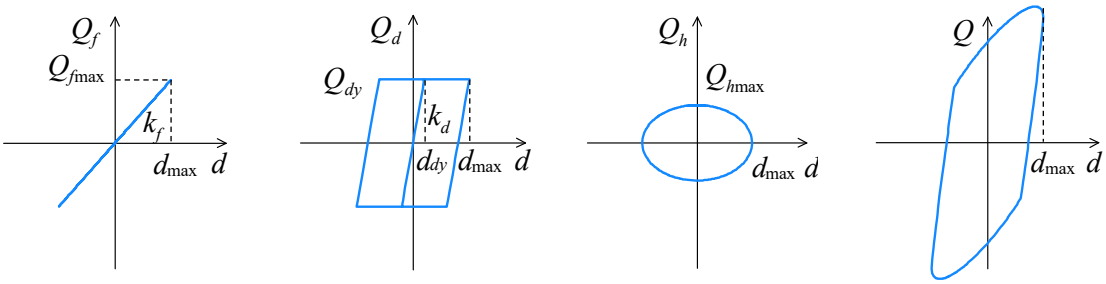

(a) Isolator (b) Hysteretic damper (c) Viscous damping (d) System

Fig. 2 Restoring Force Characteristic of system

The parameters of system can be calculated from following Eq. (1) to Eq. (6).

$$k_f = \frac{4\pi^2}{T_f^{\,2}} M \tag{1}$$

$$k_d = \frac{Q_{dy}}{\delta_{dy}}, \quad Q_{dy} = \alpha_{dy} \cdot Mg \tag{2), (3}$$

$$c_f = \frac{2h_f \cdot k_f}{\omega_f}, \quad \omega_f = \frac{2\pi}{T_f} \tag{4), (5)}$$

$$k_0 = k_f + k_d \tag{6}$$

Here, k_d : the stiffness of hysteretic damper, c_f : the viscous damping coefficient, h_f : damping ratio of isolation layer, ω_f : the natural circular frequency, and k_0: the stiffness of system.

In this paper, it is assumed that the base isolation structure model with a viscous damping and installs type hysteretic damper in the seismic isolation layer. Table 1 shows the parameters of the model. Mass M : 100 tons, T_f : period of isolator, h_f: damping ratio of isolation layer, α_{dy} : yield shear force coefficient of hysteretic damper.

Table 1 Parameters of model

Period of isolator T_f (s)	2.0, 3.0, 4.0
Damping ratio of isolation layer h_f	0.02, 0.04, 0.10
Mass M (ton)	100
Yield shear force coefficient of hysteretic damper α_{dy}	0.02, 0.03
Yield deformation of hysteretic damper δ_{dy} (cm)	3

2.2 OUTLINE OF INPUT GROUND MOTIONS

The artificially generated earthquake ground motions created to match the announcement spectrum are used as the input ground motions, and ${}_pS_v$ was set as constant at a corner period $T_C > 0.64$ s. In this paper, ART KOBE 80 cm/s and ART HACHI 80 cm/s are adopted as the ground motions. ART KOBE is artificially generated pulse-like ground motion, and ART HACHI is artificially generated long period ground motion.

Figure 3 shows the acceleration time history of the ground motions.

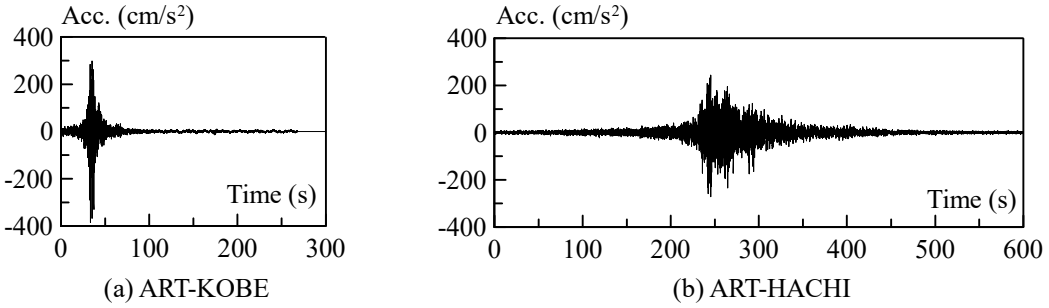

Figure 3 Earthquake Ground Motion (${}_pS_v$ = 80 cm/s)

Figure 4 shows the pseudo-velocity response ${}_pS_v$ (h = 0.05) and energy spectrum V_E = 120 cm/s (h = 0.10). And the ground motion levels are 0.2, 0.5, 0.8, 1.0 1.5 and 2.0 times. Fig. 4 shows the case where ${}_pS_v$ was constant at 80 cm/s. In this analysis, the velocity conversion value of the total input energy in ART KOBE, V_E = 118, 89, and 108 cm/s, when Period of isolator T_f = 2, 3, 4s. In ART HACHI, V_E = 218, 183, and 247 cm/s, when Period of isolator T_f = 2, 3, 4s.

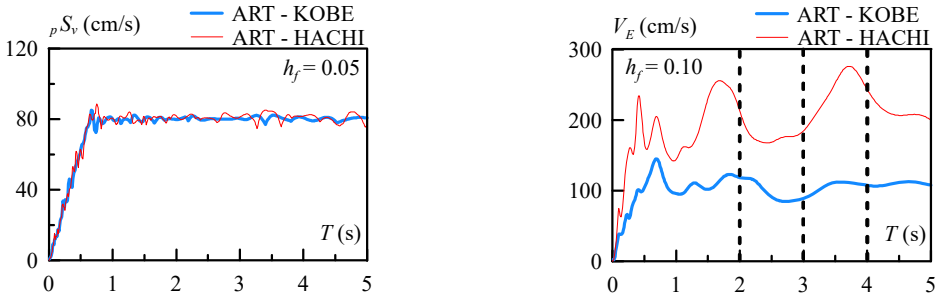

(a) Pseudo-velocity response spectrum (b) Energy spectrum

Figure 4 Earthquake ground response spectrum

3. ACCURACY OF PREDICTION METHOD FOR V_D

3.1 V_D CALCULATED BY TIME HISTORY ANALYSIS

Eq. (7) shows the equation of motion for the system:

$$m\ddot{x}(t)+c\dot{x}(t)+kx(t)+F_d(t)=-m\ddot{z}_0(t) \tag{7}$$

Here, m : Mass, $c\dot{x}(t)$: Damping force, $kx(t)$: Restoring Force, $-m\ddot{z}_0(t)$: Ground motion force
$F_d(t)$: Hysteretic damper force
Multiplied by $dx=\dot{x}(t)dt$ on both sides, and integrated over the entire duration of an earthquake, to, Eq. (8) is reduced to

$$\int_0^{t_0} m\ddot{x}(t)\dot{x}(t)dt+\int_0^{t_0} c\dot{x}(t)^2dt+\int_0^{t_0} kx(t)\dot{x}(t)dt+\int_0^{t_0} F_d(t)\dot{x}(t)dt=-\int_0^{t_0} m\ddot{z}_0(t)\dot{x}(t)dt \tag{8}$$

The item on the right side of the energy balance formula is the total input energy $E(t)$.
Eq. (9) shows the total input energy $E(t)$.

$$E(t)=-\int_0^{t_0} m\ddot{z}_0(t)\dot{x}(t)dt \tag{9}$$

The first item on the left side of the energy balance formula is the kinetic energy of the sum of isolation layer $W_{fk}(t)$ and hysteretic damper $W_{dk}(t)$ at the instant when the earthquake motion vanishes.
Eq. (10) shows the kinetic energy of the sum of isolation layer $W_{fk}(t)$ and hysteretic damper $W_{dk}(t)$.

$$W_{fk}(t)+W_{dk}(t)=\int_0^{t_0} m\ddot{x}(t)\dot{x}(t)dt=\frac{1}{2}m\dot{x}(t)^2 \tag{10}$$

The second item on the left side of the energy balance formula is the energy consumed by damping $W_{fh}(t)$.
Eq. (11) shows the energy consumed by damping $W_{fh}(t)$.

$$W_{fh}(t)=\int_0^{t_0} c\dot{x}(t)^2dt \tag{11}$$

The third item on the left side of the energy balance formula is the elastic strain energy of the sum of isolation layer $W_{fs}(t)$ and $W_{ds}(t)$ hysteretic damper[2].
Eq. (12) shows plastic hysteresis energy of elastic strain energy of the sum of isolation layer $W_{fs}(t)$.

$$W_{fs}(t) = \int_0^{t_0} kx(t)\dot{x}(t)\,dt = \int_0^{t_0} kx(t)\frac{dx(t)}{dt} = \int_0^{x(t_0)} kx(t)dx = \frac{1}{2}kx(t)^2 \tag{12}$$

The fourth item on the left side of the formula is the plastic hysteresis energy of the hysteretic damper $W_d(t)$.
Eq. (13) shows the energy of the hysteretic damper.

$$W_{de}(t) + W_d(t) = \int_0^{t_0} F_d(t)\cdot\dot{x}(t)\,dt \tag{13}$$

The kinetic energy W_k and the elastic strain energy W_s constitute the elastic vibrational energy, W_e, $W_{de}(t)$ and $W_d(t)$ represent the elastic vibration energy and plastic hysteresis energy of the hysteretic damper, respectively. So, the energy balance formula can be showed as Eq. (14).

$$W_{fe}(t) + W_{de}(t) + W_{fh}(t) + W_d(t) = E(t) \tag{14}$$

Figure 5 shows the historic response of energy. The horizontal axis shows the starting time of earthquake as t. Here, t_m and t_0 represent the maximum response value occurring time of a building and duration of the earthquake motion. It can be observed from Figure 5 that $W_{fe}(t)$, $W_{de}(t)$ exhibited maximum values at $t = t_m$ and almost disappeared at $t = t_0$.

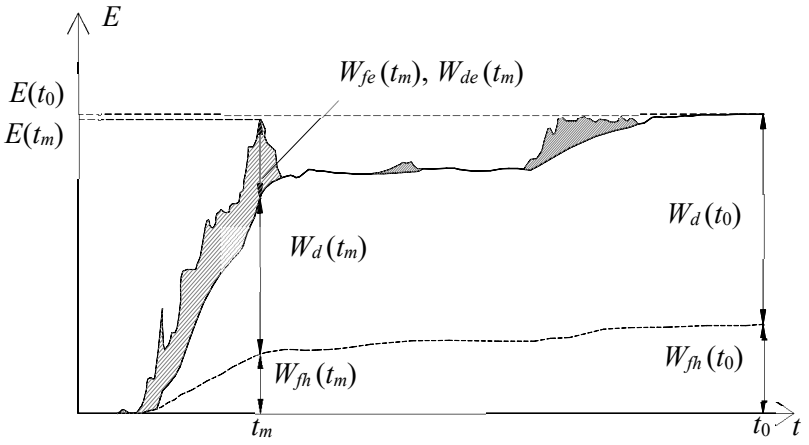

Figure 5 Historic response of energy

Further, $E(t)$ represents the input energy, and $E(t) - W_{fh}(t)$ is defined as the energy $E_D(t)$ that contributed to the damage [2]. In this study, we considered the energy balance by focusing on the maximum response value generation time t_m. In the isolation structure with hysteretic damper, it can be observed that $E(t_m) < E(t_0)$. When $t = t_0$, $W_{fe}(t_m)$ and $W_{de}(t_m)$ can be ignored, as it is significantly smaller than $E_D(t_0)$. If $E_D(t_0)$ is replaced with $E_D(t_m)$ in the isolation structure, the formula for $t = t_0$ can be expressed as follows:

$$E_D(t_0) = W_d(t_0) \tag{15}$$

The equation for the total energy input is expressed by an equivalent velocity V_E is as follows [2]:

$$V_E = \sqrt{\frac{2E(t_0)}{M}} \tag{16}$$

The equation for the energy input that contributes to damage is expressed by an equivalent velocity V_D is as follows [2]:

$$V_D = \sqrt{\frac{2E_D(t_0)}{M}} \tag{17}$$

3.2 V_D CALCULATED BY PREDICTION METHOD

According to earthquake ground response spectrum showed in Figure 4(b), the V_E(Per.) can be calculated.

Eq. (18) [2] shows the relationship between V_E and V_D. And the equation proposed by Akiyama[2]. So, V_D (Per.) is calculated using the following equation.

$$\frac{V_D}{V_E} = \frac{1}{1+3h_f+1.2\sqrt{h_f}} \tag{18}$$

Accuracy of this formula can be verified by comparing with results of time history analysis showing in subchapter 3.1.

3.3 ACCURACY OF V_D

Figure 6 shows the relationship between V_E (Pre.) and V_E (THA), (a) shows the results of ground motion ART KOBE, and (b) shows the results of ground motion ART HACHI. Here, V_E (Pre.) is calculated by Fig. 5, V_E (THA) is calculated by Eq. (16), and error is V_E (Pre.)/ V_E (THA) from 10% to 50%. When α_{dy} = 0.02 and α_{dy} = 0.03, the legends are red and blue; △, □, and ○ show the damping ratio h_f = 0.02, 0.04 and 0.10; blank, filling, and patterns show period of isolator T_f = 2, 3 and 4s, respectively.

The accuracy of V_E(Pre.) / V_E(THA) can be observed from Fig. 6, for ART KOBE, almost error of cases less than 20%, and most of cases less than 15%. For ART HACHI, almost all error of all cases less than 15%, and almost cases less than 10%. In addition, the larger ground motion is, the better the accuracy is.

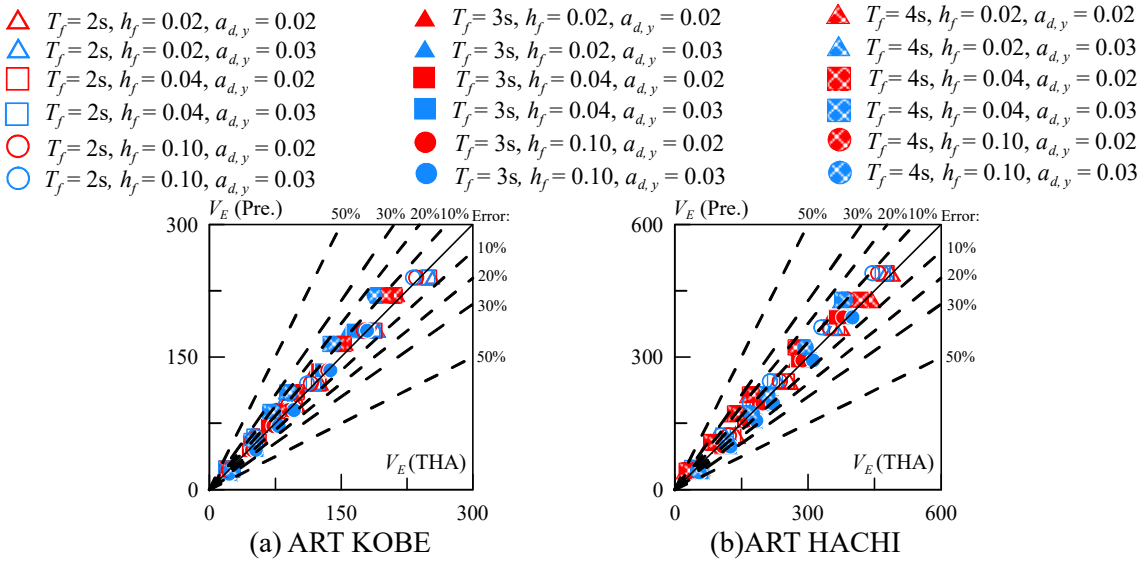

Figure 6 Relationship between V_E (Pre.) and V_E (THA)

Fig. 7 shows the relationship between V_D (Pre.) and V_D (THA), (a) shows the results of ground motion ART KOBE, and (b) shows the results of ground motion ART HACHI. Here, V_D (Pre.) is calculated by Eq. (18), V_D (THA) is calculated by Eq. (17), and error is V_D (Pre.)/ V_D (THA) from 10% to 50%. When $\alpha_{dy} = 0.02$ and $\alpha_{dy} = 0.03$, the legends are red and blue; △, □, and ○ show the damping ratio $h_f = 0.02$, 0.04 and 0.10; blank, filling, and patterns show period of isolator $T_f = 2$, 3 and 4s, respectively.

It can be observed from Fig. 7 that the larger ground motion is, the better the accuracy is. The accuracy of V_D(Pre.) and V_D(THA) can be observed from Fig. 7, for ART KOBE, almost error of cases less than 25%, and most of cases less than 15%. For ART HACHI, almost error of all cases less than 20%, and almost cases less than 10%.

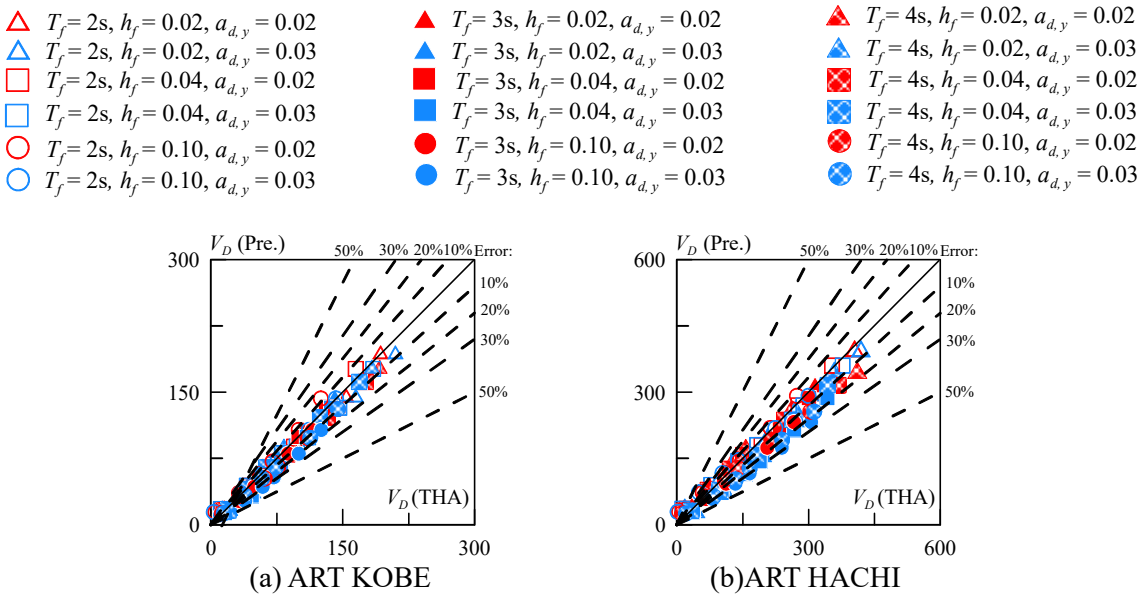

Figure 7 Relationship between V_D (Pre.) and V_D (THA)

Figure 8 shows the relationship between V_D / V_E (THA) and plastic ductility ratio $\mu_d = \delta_{\max} / \delta_{dy}$. Fig. (a) shows the results of ground motion ART KOBE, and Fig. (b) shows the results of ground motion. (i) shows the results of the damping ratio h_f=0.02, (ii) shows the results of the damping ratio h_f=0.04, and (iii) shows the results of the damping ratio h_f=0.10. Here, V_D / V_E (THA) is calculated by Eq. (16) and Eq. (17). Horizonal broken lines show V_D / V_E (Pre.) calculated by Eq. (18), when $h_f = 0.02$, 0.04 and 0.10, V_D / V_E (Pre.) = 0.81, 0.74 and 0.60. Here, $\delta_{\max}$ shows maximum deformation of hysteretic damper and δ_{dy} shows yield deformation of hysteretic damper. When $\alpha_{dy} = 0.02$ and $\alpha_{dy} = 0.03$, the legends are red and blue; △, □, and ○ show the damping ratio $h_f = 0.02$, 0.04 and 0.10; blank, filling, and patterns show period of isolator $T_f = 2$, 3 and 4s, respectively.

Figure 8 shows arrange of plastic ductility ratio. For ART KOBE, μ_d = 1.06 – 28.64. For ART HACHI, μ_d = 1.00 – 22.33. When the earthquake is comparatively small, $\mu_d \approx 1$, the model is in the elastic state for most of the time, and the plastic deformation is exceedingly small, so the plastic energy consumption is small. And it can be observed that when the plastic ductility ratio μ_d is large enough, the accuracy tends to be stable.

According to Fig. 8, as for almost cases, the error, (V_D / V_E (THA)) / (V_D / V_E (Pre.)), is decreased with decreasing the damping ratio h_f, the error is decreased with decreasing α_{dy} and the error is decreasing with decrease of T_f.

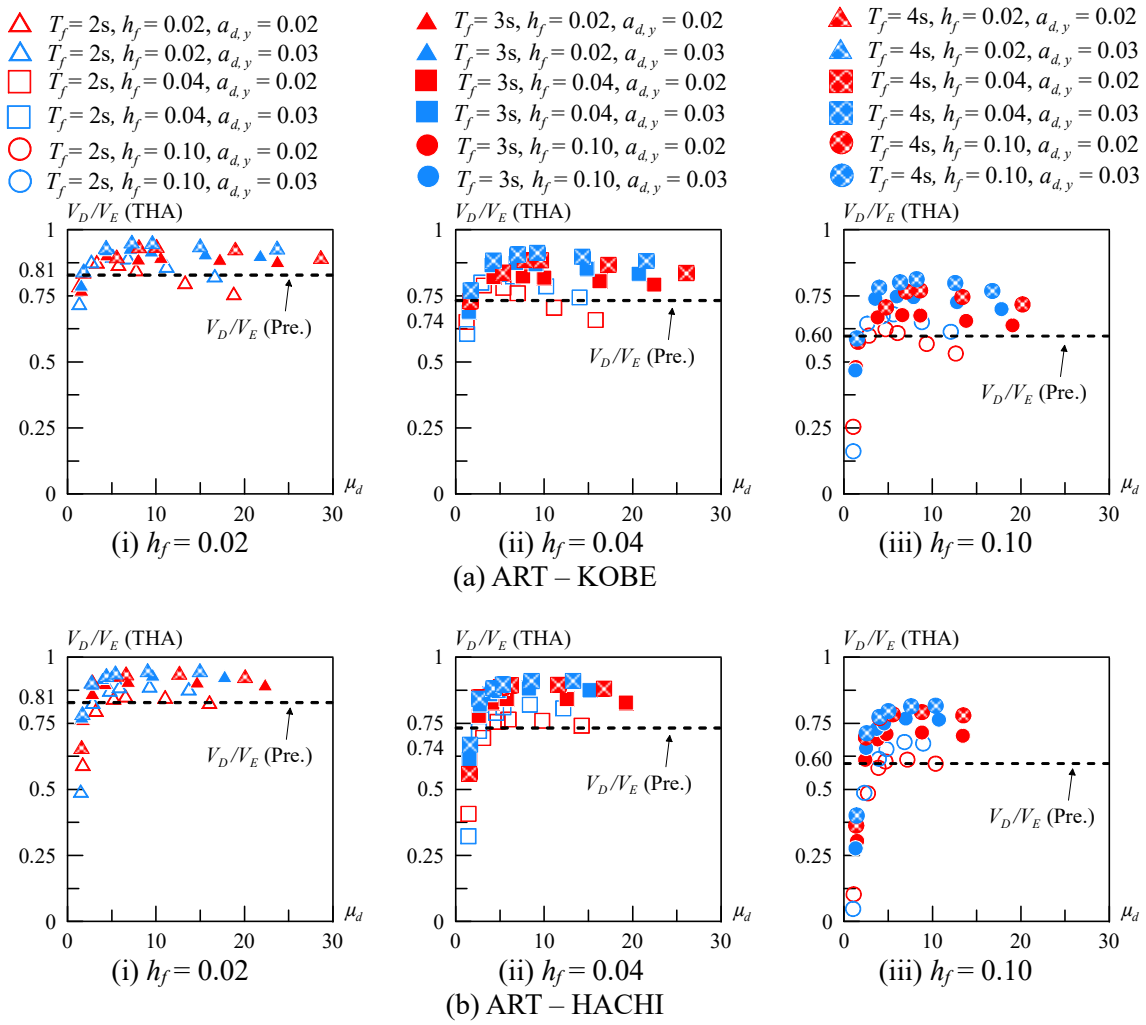

Fig. 8 Relationship between V_D/V_E (THA) and μ_d

4. CONCLUSIONS

The propose of this paper is to discuss accuracy of prediction formula for energy caused by hysteretic damper. The artificially generated earthquake ground motions are be adopted to calculate the response of a SDOF isolation structure by time history analysis.

According to research of this paper we know that:

(1) The accuracy of the equivalent velocity calculated by Eq. (16) V_E(THA) is satisfactory, for ART KOBE, almost error of cases less than 20%, and most of cases less than 15%. For ART HACHI, almost all error of all cases less than 15%, and almost cases less than 10%.

(2) The accuracy of the equivalent velocity calculated by Eq. (17) V_D(THA) is satisfactory, for ART KOBE, almost error of cases less than 25%, and most of cases less than 15%. For ART HACHI, almost all error of all cases less than 20%, and almost cases less than 10%.

(3) V_D / V_E (THA) tends to stabilize with increasing the plastic ductility ratio μ_d.

(4) As for almost cases, the error of V_D / V_E (THA) is decreased with decreasing the damping ratio h_f, the error is decreased with decreasing α_{dy} and the error is decreased with decreasing the period of isolator T_f.

According to this paper, verification of the proposed theory indicates good accuracy for artificially generated earthquake ground motions.

ACKNOWLEDGMENT

This work was supported by JST Program on Open Innovation Platform with Enterprises, Research Institute and Academia (JPMJOP1723).

REFERENCES

1) HIROSHI Akiyama：Earthquake Resistant Design for Buildings based on Energy Balance，1999 (in Japanese)
2) KITAMURA　Haruyuki：Seismic Response Analysis Methods for Performance Based Design, 2nd，2009 (in Japanese)
3) NAOSHI Nomura，DAIKI Sato，KITAMURA　Haruyuki：Response Prediction Method for Flexible- Stiff Mixed Structure with Displacement Controller Based on Energy Balance, AIJ，NO.692，pp.1705-1713, 2013.10 (in Japanese)